

PtNi AND CoNi FILM ELECTROCATALYSTS PREPARED BY MOCVD FOR THE OXYGEN REDUCTION REACTION IN ALKALINE MEDIA.

M.A. García-Contreras^{1*}, S.M. Fernández-Valverde¹, J.R. Vargas-García²

¹Departamento de Química, Instituto Nacional de Investigaciones Nucleares, C.P. 52045 México

²Departamento de Ing. Metalúrgica, ESIQIE-IPN, C.P. 07300, México, D.F.

*Tel.: +52 553297200 x2280; fax: +52 553297301, miguel.garcia@inin.gob.mx

Abstract

CoNi and PtNi film electrocatalysts were prepared by Metal-Organic Chemical Vapour Deposition (MOCVD) and their electrocatalytic activity for the oxygen reduction reaction (ORR) in 0.5 M KOH was investigated by cyclic voltammetry and Rotating Disk Electrode techniques. Experiments included working electrodes of Co, Ni and Pt obtained also by MOCVD for comparison. The film electrocatalysts were characterized by X-ray diffraction, Scanning Electronic Microscopy and Energy dispersive X-ray analysis. Films thickness were about 200-250 nm and nanocrystalline particles were found in the range of 12 to 30 nm. In the same experimental conditions, the overpotential for the ORR at a current density of 1 mA cm⁻² for PtNi film is 175 mV lower than the overpotential of Pt film electrocatalyst. An enhanced activity was observed on PtNi with respect to Pt. The electrochemical response for the oxygen reduction reaction on CoNi film is higher than those of elemental Ni and Co films obtained by MOCVD.

1) Introduction

The search for good electrocatalysts to be used as cathodes in Fuel Cells for the oxygen reduction reaction is still a major challenge. A good electrocatalyst to be considered for being used in Fuel Cells should have a potential close to the equilibrium potential (0.401 V at 25 °C in alkaline media) at an established current density [1]. Extensive research has focused on the study of oxygen reduction in acid media; still acid electrolytes are mainly used in fuel cell systems [2]. However, alkaline fuel cells using liquid electrolyte solutions of potassium or sodium hydroxide have advantages over all other fuel cells technologies due to their long lifetime, the possibility of using non-noble catalysts and faster kinetics for the oxygen reduction reaction (ORR) [3,4]. For the ORR, platinum is the leader metal. Cobalt-platinum and nickel-platinum alloys have shown interesting catalytic properties for the ORR in acid media [5-10] and a study has

been done with PtCo in alkaline media [11]. Some researchers have reported a series of factors responsible of the higher performance for the ORR using catalysts with platinum alone or in binary, tertiary metals or alloy surfaces and bimetallic combinations, investigated by spectroscopic studies [12-17]. Such factors are changes in the Pt-Pt bond distance, the number of Pt nearest neighbors, the electron density in the Pt 5d orbital, the presence of surface oxide layers and surface roughness effects. For thin Pt films it has been found that oxygen reduction activity depends on the grain size, specific surface area and lattice parameter [18]. For PtCo and PtNi alloys it has been reported a higher activity for the ORR than Pt alone associated with reduced Pt-Pt neighboring distance which seems to be favorable for the adsorption of oxygen [9]. These reported electrocatalysts have been prepared in situ by incipient wetness, sputtering, etc. and other were acquired from suppliers (E-TEK Corporation, Johnson-Matthey, Inc. USA, Hauner GmbH, Germany).

Thin films have been prepared by several deposition techniques such as spray pyrolysis [19], RF-sputtering [20], CVD (Chemical Vapor Deposition) [21-26], electrodeposition [27,28], pulsed laser deposition (PLD) [29], sol-gel process [30], and spin coating [31] on a variety of substrates. Among these techniques, CVD offers several advantages such as uniform deposition over large area, conformal coverage and selective deposition. Also, CVD has the advantage over other techniques to produce materials with size in nanometer scale.

CVD is by definition a chemical process and some parameters, such as reaction temperature, reactor pressure and chemistry of the precursor material, as well as the nature of the substrate, affect film growth and microstructure. Films prepared by CVD usually have applications in electronic, optoelectronic industry, for resistant coating against corrosion and wear [32]. However, there have been several proposals to prepare catalysts by using the CVD process where nanometric materials with a high surface area to volume ratio are required. Only some groups of researchers have worked to prepare catalysts with noble metals by CVD due to attractive results that these nanomaterials have shown and because of the advantages of CVD upon conventional methods to prepare electrocatalysts [32]. If the precursors used for the Chemical Vapor Deposition are metal-organic materials, the technique is called MOCVD and has the advantage over CVD that process temperatures are lower than those employed in CVD.

The objective of this study was to use the MOCVD technique to prepare film electrocatalysts of CoNi, PtNi, Co, Ni and Pt to evaluate their performance for the oxygen reduction reaction in 0.5 M KOH.

2) Experimental

CoNi and PtNi films as well as Co, Ni and Pt films were prepared on amorphous glass slides (2 cm length, 1 cm wide and 0.1 cm thick) and glassy carbon rods (0.5 cm in diameter and 1.0 cm length) in a horizontal hot-wall MOCVD apparatus reported before [32] using metal-acetylacetonates as precursors [33]. Prior to deposition, the glassy carbon rods were wet-abraded up to 1000 grit emery paper, ultrasonically cleaned in acetone, distilled water and isopropanol and then dried. The best reaction conditions determined experimentally for the deposition of the of metallic films were as follows; briefly, the precursors were mechanically mixed in 1:1 weight ratio and evaporated together at 460-545 K, the vapors were carried to the reactor chamber using argon gas at a constant flow rate of 180 sccm. The deposition temperature (T_{dep}) was varied from 673 to 723 K and total pressure (P_{tot}) was kept constant at 1 torr. Depositions were performed for 20 min. Films crystalline structure was investigated by X-ray diffraction (XRD, Siemens D5000 diffractometer) using a monochromatic Cu- $K\alpha_1$ radiation and the average crystallite size was estimated by the Scherrer equation using the (111) plane [34]. Micrographs were obtained by scanning electron microscopy (JEOL JSM-6300) and chemical analysis of films was carried out by energy dispersive X-ray analysis (EDAX). The electrocatalytic activity of the elemental and bimetallic films was investigated in a 0.5 M KOH solution at room temperature by cyclic and linear voltammetry. A typical three-electrode electrochemical cell was coupled to a potentiostat/galvanostat EG&G PAR model 273A and a rotating disk electrode (RDE). Films deposited on the cross-section of the glassy carbon rods (geometric area: 0.196 cm²) were used as working electrodes, reference electrode was Hg/HgO (0.194 V vs. NHE) and a platinum gauze was employed as counter electrode. The cyclic voltammetry was performed at 50 mVs⁻¹, all curves reported are those for the 50th cycle after which subsequent changes in voltammograms become negligible. Prior to the measurements, N₂ was bubbled through the solution during 30 minutes. After electrode activation, electrolyte solution was saturated with high purity oxygen and RDE measurements were performed at a scan rate of 20 mV s⁻¹ with a rotation speed of 100-1600 rpm. An oxygen atmosphere was maintained over the electrolyte solution during

RDE experiments and temperature was kept constant at 298 K. All potentials reported in this study are referred to the Normal Hydrogen Electrode (NHE).

3) Results and discussion

Table 1 presents particle size, thickness and EDAX analysis of the films deposited by MOCVD. As expected, particle size is lower than 100 nm for all deposited samples, in accordance with those merits mentioned about CVD process. Film thickness is in the range of 200-250 nm in accordance with reported values elsewhere (150-300 nm) [35]. As the top surface of a film becomes oxidized due to exposure to air, the EDAX analysis shows the presence of oxygen in all films, except for platinum. In the limits of EDAX technique for Ni, a NiO surface can be deduced. In all other films a mixture of oxides should be present. Paranjape et al. [35] reported for cobalt deposits in similar conditions that there is a surface layer (extending 5 nm or slightly more) revealed as an oxide layer by Secondary Ion Mass Spectrometry (SIMS).

Table 1. Particle size, thickness and EDAX analysis of films deposited by MOCVD

film	particle size nm	thickness nm	EDAX analysis atomic %
Co	28	190	Co 34 O 66
Ni	29	240	Ni 50 O 50
CoNi	12	225	Co 21 Ni 32 O 47
Pt	30	240	Pt 100
PtNi	18	210	Pt 28 Ni 27 O 45

Fig. 1 shows XRD patterns of Co, Ni and CoNi films. It can be observed widened reflections indicating nanometric size. DRX patterns were compared with Powder Diffraction Files 15-0806 and 04-0850.

Fig. 2 shows SEM images of MOCVD films. Fig. 2a) is a typical cross-sectional SEM image of a Ni film at 20000X deposited on a glass slide, the thickness of the film is approximately 240 nm. Micrograph b) of Fig. 2 shows a SEM image of PtNi film at 1000X upon glassy carbon, it has a rough surface with the shape of the carbon substrate used for the deposition. Micrograph c) corresponds to the image of a Ni film deposited

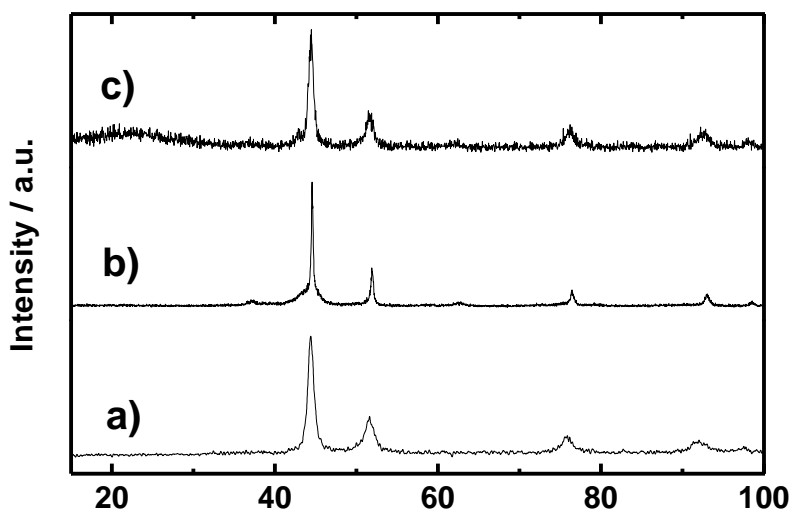


Fig. 1 DRX patterns of a)Co b) Ni and c) CoNi films.

upon glassy carbon; in this figure particles from 120 to 175 nm in size are observed. Other images of CoNi and Pt films (not shown) also displayed roughed surfaces. It has been reported that the resulting film shape is influenced by the type of substrate, i.e. different substrates can lead to very different microstructures [34]. In this work the glassy carbon substrates were only polished as reported before and it was observed that the surface roughness of the films was influenced consequently.

Fig. 3 shows cyclic voltammograms of Pt and PtNi films in alkaline media. The Pt cyclic voltammograms is typical with two hydrogen adsorption peaks at -0.4 and -0.5 V vs. NHE, a desorption hydrogen peak at -0.56 V and the Pt oxide reduction peak at 0.0 V. The cyclic voltammogram of PtNi film is similar to the one of Pt film, but the adsorption hydrogen peaks are very smoothed and shifted to more positive potentials. This could be attributed to the presence of nickel and differences in the oxidation state of the film electrodes.

Fig. 4 shows cyclic voltammograms of Co, Ni and CoNi films in 0.5 M KOH. Only a few peaks of redox reactions are observed on each surface film. The Co film has an anodic peak at *ca* 0.2 V which represents the formation of the Co(II) hydroxide, according to Pourbaix [36] and Burke et al.[37,38] the Co(OH)₂ should be formed before CoO. The cathodic peak at *ca* -0.09 V is the hydroxide reduction. The Ni film has a cathodic peak

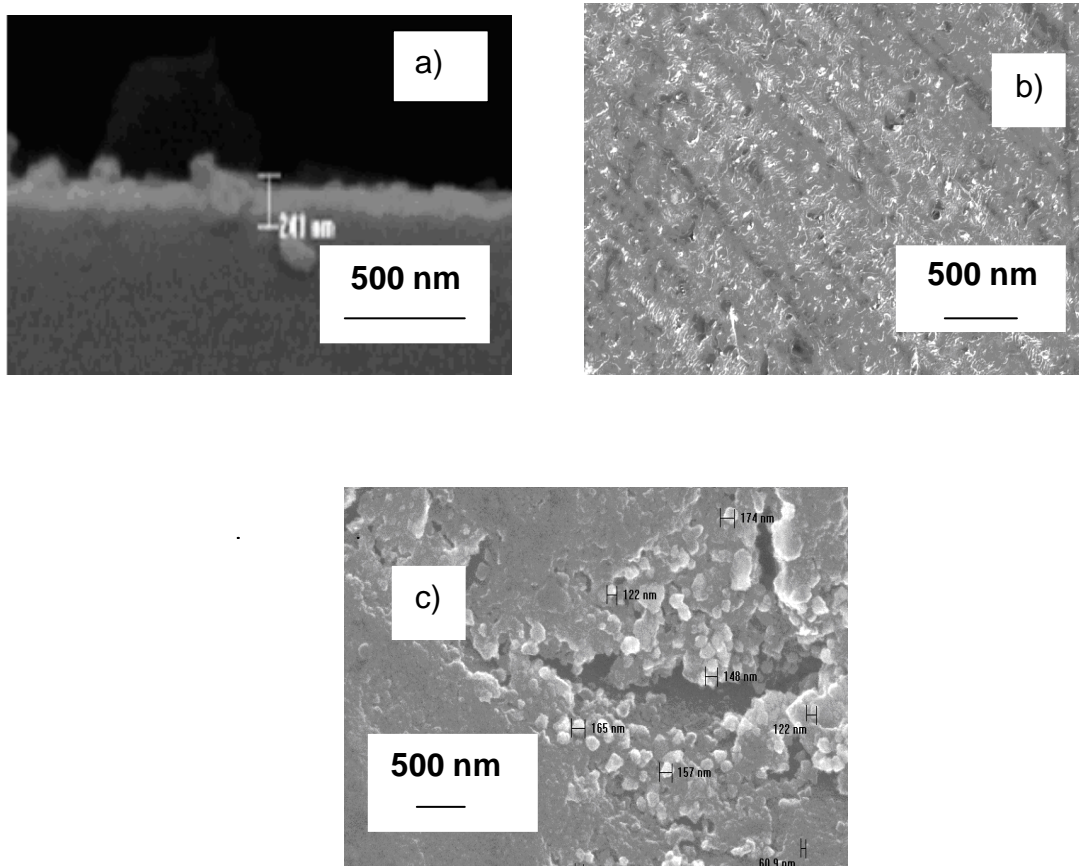


Fig. 2 SEM images of MOCVD films; a) Cross-sectional view of on glass slide, b) PtNi on glassy carbon, c) Ni on glassy carbon

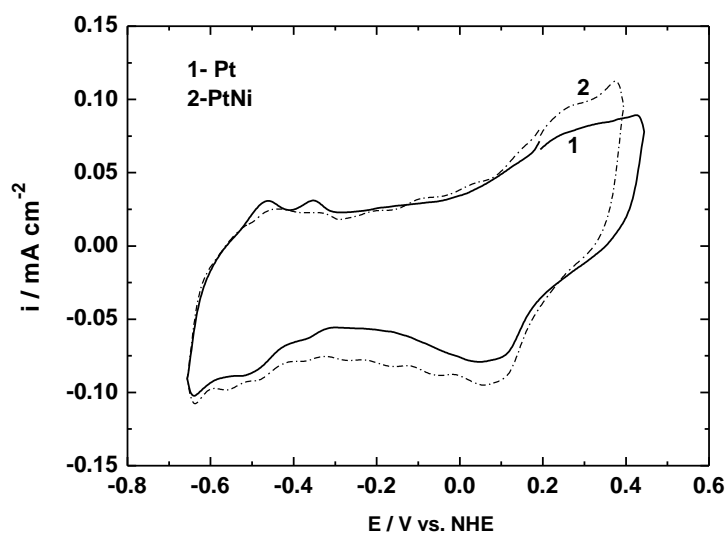


Fig. 3 Cyclic voltammograms for Pt and PtNi films in N_2 -saturated 0.5 M KOH at a sweep rate of 50 mV s^{-1} .

at *ca* -0.1 V corresponding to the reduction of nickel oxides to Ni(OH)₂ as reported elsewhere [36].

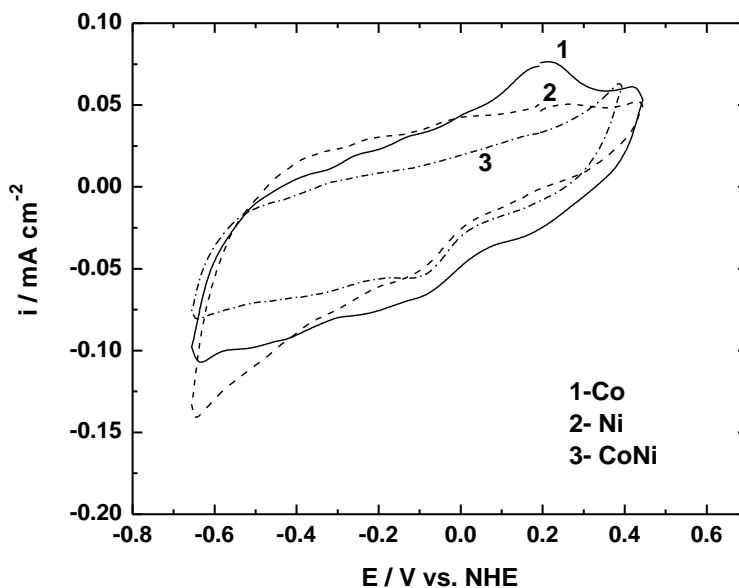


Fig. 4 Cyclic voltammograms for Co, Ni and CoNi films in 0.5 M KOH.

To evaluate the performance for the oxygen reduction reaction of the MOCVD films, typical polarization curves were obtained at six rotation frequencies, between 100 and 1600 rpm, with a scan rate of 20 mV s^{-1} in a 0.5 M KOH oxygen saturated solution. The rotational speed increased the limiting currents due to the high oxygen diffusion to the electrode surface. Fig. 5 presents the rotating disk electrode data for oxygen reduction on the Pt MOCVD film.

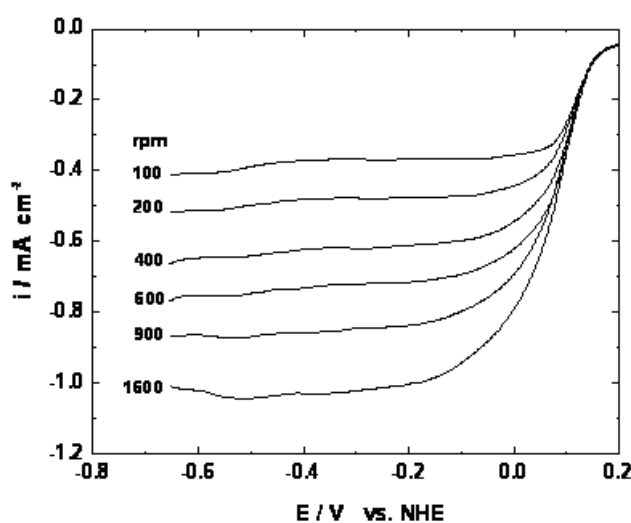


Fig. 5 Voltammetry curves for oxygen reduction on Pt film in O₂-saturated 0.5 M KOH at a sweep rate of 20 mV s^{-1} .

Fig. 6 shows standard polarization curves for the oxygen reduction reaction on rotating disk electrodes of PtNi and CoNi films at 1600 rpm in 0.5 M KOH oxygen saturated at 25 °C. Pt, Co, and Ni films are included, as well as Co and Ni rods for comparison.

CoNi film showed a higher current density than Co and Ni films obtained by MOCVD, and its onset potential for ORR is shifted to more positive potentials, although only for 40 mV. This performance could be attributed to a synergetic effect from the CoNi alloy formation.

PtNi film shows a higher activity for the ORR than Pt film and a lower overpotential at a current density of 1 mAcm⁻² of 175 mV at 1600 rpm. This overpotential value is lower than others reported in the literature. For example, Toda *et al.* reported a lower overpotential of 150 mV on sputtered PtNi in 0.1 M HClO₄ [39] in relation to Pt prepared at the same conditions. Drillet et al. found a reduction of about 80 mV for a PtNi disc electrode in H₂SO₄/CH₃OH solution [40] also compared to Pt disc obtained at the same experimental conditions. Pt film shows a small decay of current at high overpotential, prior to the hydrogen evolution reaction. Evidently, the number of surface sites which are needed for O₂ to undergo reduction is decreasing due to hydrogen electrosorption [41].

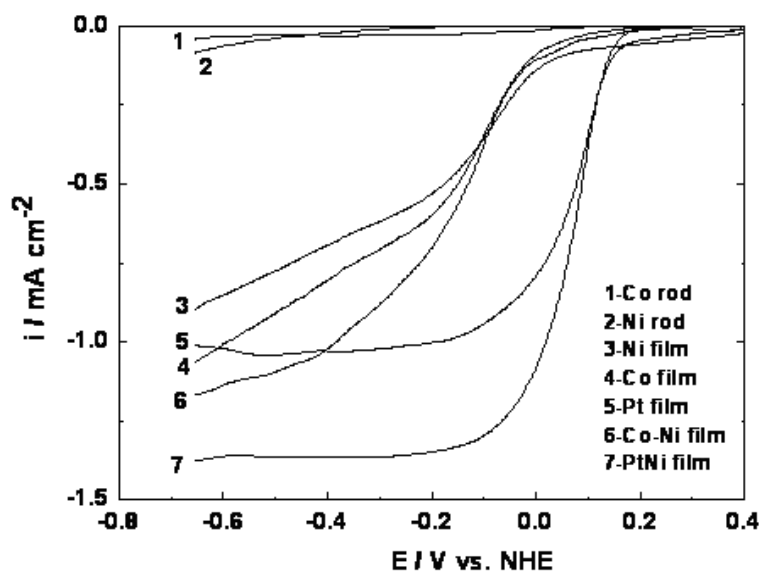


Fig. 6 Polarization curves on rotating disk electrodes of Pt, Co, Ni, CoNi and PtNi films at 1600 rpm in 0.5 M KOH saturated with oxygen at 25 °C.

4) Conclusions

PtNi and CoNi films prepared by metal-organic chemical vapor deposition showed to be crystalline and with nanometric size. PtNi and CoNi had a surface oxide layer according to EDAX. CoNi film showed a higher current density than Co and Ni films obtained by MOCVD, and its onset potential for ORR is shifted to more positive potentials. PtNi film electrode showed the lowest overpotential and the highest current density for the oxygen reduction reaction in KOH 0.5 M among all electrocatalysts prepared by MOCVD in this study.

5) Acknowledgements

This work was supported by ININ through project ININ-CB-906. The assistance given by L. Carapia in SEM images and EDAX analysis is gratefully acknowledged. The authors would also like to thank M. Espinosa and I. Martínez for assisting with the XRD analysis.

6) References

- [1] E. Yeager, *Electrochim. Acta*, 29, 1527, (1984).
- [2] *Fuel Cell Handbook*, 4th ed., US Department of Energy, (1998).
- [3] Y. Kiros, S. Schwartz, *J. Power Sources*, 36, 547, (1991).
- [4] Y. Kiros, O. Lindstrom, T. Kaimakis, *J. Power Sources*, 45, 219, (1993).
- [5] L. Geniès, R. Faure, R. Durand, *Electrochim. Acta*, 44, 1317, (1998).
- [6] T. Toda, H. Igarashi, H. Uchida, M. Watanabe, *J. Electrochem. Soc.*, 146, 3750, (1999).
- [7] Y Kiros, *J. Electrochem. Soc.*, 7, 2152, (1996).
- [8] M. Min, J. Cho, K. Cho, H. Kim, *Electrochim. Acta*, 45, 4211, (2000).
- [9] M. D. Obradovic, B. N. Grgur, Lj.M. Vracar, *J. Electroanal. Chem.*, 548, 69, (2003).
- [10] M. Watanabe, K. Tsurumi, T. Mizukami, T. Nakamura, P. Stonehart, *J. Electrochem. Soc.*, 141, 2659, (1994).
- [11] Fabio H. B. Lima, Edson A. Ticianelli, *Electrochim. Acta*, 49, 4091, (2004).
- [12] T. Toda, H. Igarashi, M. Watanabe, *J. Electroanal. Chem.*, 460, 258, (1999).
- [13] A. S. Arico, A. K. Shukla, H. Kim, S. Park, M. Min, V. Antonucci, *Appl. Surf. Sci.*, 172, 33, (2001).

- [14] A. K. Shukla, M. Neergat, P. Bera, V. Jayaram, M. S. Hedge, *J. Electroanal. Chem.*, 504, 111, (2001).
- [15] S. Mukerjee, S. Srinivasan, M. P. Soriana, J. McBreen, *J. Phys. Chem.*, 99, 4577, (1995).
- [16] J. Cho, W. Roh, D. Kim, J. Yoon, J. Choy, H. Kim, *Faraday Trans.*, 94, 2835, (1998).
- [17] K. Kinoshita, in: *Electrochemical Oxygen Technology*, vol. 19, Wiley, New York, (1992).
- [18] J. A. Poirier, G. E. Stoner, *J. Electrochem. Soc.*, 141, 42, 5, (1994).
- [19] P. S. Patil, L. D. Kadam, C. D. Lokhande, *Thin Solid Films*, 272, 29, (1996).
- [20] J. G. Cook, M. P. van der Meer, *Thin Solid Films*, 144, 165, (1986).
- [21] E. Fujii, H. Torii, A. Tomozawa, R. Takayama, T. Hirao, *J. Mater. Sci.*, 30, 6013, (1995).
- [22] D. Barreca, C. Massignan, S. Daolio, M. Fabrizio, C. Piccirillo, L. Armelao, E. Tondello, *Chem. Mater.*, 13, 588, (2001).
- [23] T. Maruyama, T. Nakai, *Sol. Energy, Mater.*, 23, 25, (1991).
- [24] K. Shalini, A. U. Mane, S. Choopun, M. Rajeswari, S. A. Shivashankar, *J. Crystal Growth*, 231, 242, (2000).
- [25] A. U. Mane, K. Shalini, A. Wohlfart, A. Devi, S.A. Shivashankar, *J. Crystal Growth*, 240, 157, (2002).
- [26] T. Maruyama, S. aria, *J. Electrochem. Soc.*, 143, 1383, (1996).
- [27] D. Larcher, G. Sudant, J-B. Leriche, Y. Chabre, J-M. Tarrascon, *J. Electrochem. Soc.*, 149, A234, (2002).
- [28] K. Nakaoka, M. Nakayama, K. Ogura, *J. Electrochem. Soc.*, 149, C159, (2002).
- [29] R. J. Kennedy, *IEEE Trans. Magn.*, 31, 3829, (1995).
- [30] E. Barrera, T. Viveros, A. Avila, P. Quintana, M. Morales, N. Batina, *Thin Solid Films*, 346, 138, (1999).
- [31] M. Sato, H. Hara, H. Kuritani, T. Nishide, *Sol. Energy Mater. Cells*, 45, 43, (1997).
- [32] J.A. Montes de Oca, J.R. Vargas, J. Godínez, *J. Surf. Eng.*, 16, 66, (2000).
- [33] H. O. Pierson, *Handbook of Chemical Vapor Deposition*, 2nd Ed. Noyes Publications, (1999).
- [34] A. R. West, *Solid State Chemistry and Its Applications*, Wiley, New York, (1984).
- [35] M. A. Paranjape, A. U. Mane, A. K. Raychaudhuri, K. Shalini, S. A. Shivashankar,

- B. R. Chakravarty, *Thin Solid Films*, 413, 8, (2002).
- [36] M. Pourbaix, *Atlas of Electrochemical Equilibrium in Aqueous Solutions*, 2nd English edn., p. 330. NACE, Houston, (1974).
- [37] L. D. Burke, O. J. Murphy, *J. Electroanal. Chem.*, 109, 373, (1980).
- [38] L. D. Burke, M. E. Lyons, O. J. Murphy, *J. Electroanal. Chem.*, 132, 247, (1982).
- [39] T. Toda, H. Igarashi, M. Watanabe, *J. Electrochem. Soc.*, 145, 4185, (1998).
- [40] J. F. Drillet, A. Ee, J. Friedemann, R. Kötz, B. Schnyder, V. M. Schmidt, *Electrochim. Acta*, 47, 1983, (2002).
- [41] K. Tammeveski, T. Tenno, J. Claret, C. Ferrater, *Electrochim. Acta*, 42, 893, (1997).